Probing the structure of the cold dark matter halo using ancient mica

Edward A. Baltz and Andrew J. Westphal
Department of Physics, University of California, Berkeley, CA 94720-7300

Daniel P. Snowden-Ifft
Department of Physics, Occidental College, Los Angeles, CA 90041

Mica can store (for > 1 Gy) etchable tracks caused by atoms recoiling from WIMPs. Ancient mica is a directional detector despite the complex motions it makes with respect to the WIMP "wind". We can exploit the properties of directionality and long integration time to probe for structure in the dark matter halo of our galaxy. We compute a sample of possible signals in mica for a plausible model of halo structure.

arXiv:astro-ph/9711039v1 5 Nov 1997

It has been shown that 90% of the mass of our galaxy is in a halo whose radius is at least 50 kpc, extending far beyond the luminous matter [1]. The nature of this dark halo is still a subject of active research. One promising possibility is that this halo consists of weakly interacting massive particles (WIMPs). The theoretical support for this possibility is strong, both from theories of galaxy formation and supersymmetric extensions to the standard model [2]. There is a large experimental effort to detect these particles in the halo of our galaxy. One technique consists of searching ancient mica for damage caused by the rare WIMP interactions [3]. This technique has two advantages. The first is that the integration time can be of order 1 Gy if suitably old mica is chosen for study. This is unique in that the mica samples the halo continuously along the galactic orbit. The second is that mica exhibits a directional sensitivity when used as a WIMP detector [4,5]. In this work we describe how these two advantages can be used in concert to probe the structure of a WIMP halo in a way that no other dark matter experiment can.

A halo consisting of WIMPs need not have a smooth distribution in phase space as is often assumed. In the hierarchical clustering paradigm of halo formation [6], small objects form earliest, and large objects are formed by mergers between small objects. It is far from certain that the small objects are completely disrupted by these mergers. We know that there are large dark matter clumps of about $10^8 M_\odot$ in the galactic halo, the dwarf spheroidal galaxies. It is plausible that there may be other such clumps without a luminous baryonic component persisting in the halo today, providing a substantial substructure. An alternate scenario is that the clumps are being tidally disrupted. Calculations indicate that clumps can trail streamers of tidal debris along a large fraction of their galactic orbit [7].

We consider a model of the halo where a fraction f of the mass is in dense, gravitationally bound clumps or streamers and the remaining fraction is completely thermalized. The individual clumps are modeled as isothermal spheres with virial velocities of 40 km sec^{-1} and cutoff velocities of 80 km sec^{-1}, though the results of this work are insensitive to the exact values of these parameters.

A streamer looks quite similar to a clump for an observer passing through it. We model a streamer of mass M which is stretched relative to its diameter by a factor of η as being equivalent to a number η of separate clumps each with mass M/η. If we consider a halo consisting of roughly 10^4 clumps, each with mass $10^8 M_\odot$ like the dwarf spheroidals, and we assume that $\eta \sim 100$ as is shown in simulations [8], we find a halo which is effectively made from about 10^6 clumps of mass $10^6 M_\odot$.

We adopt the standard parameters for the isothermal component of the halo. The thermal velocity is 261 km sec^{-1} and the cutoff velocity is 640 km sec^{-1}. The local density of the isothermal dark matter sphere is taken to be 0.3 $(1-f)$ GeV cm^{-3} [2].

We study two density profiles for the clump fraction of the halo, those of Hernquist [9] and Navarro, Frenk, and White (NFW) [10]. Both are isotropic and are described completely by a mass parameter M and a scale radius a. The Hernquist profile has density and gravitational potential

$$\rho(r) = \frac{M}{2\pi}\frac{a}{r(r+a)^3}, \qquad \phi(r) = -\frac{GM}{r+a}, \tag{1}$$

while the NFW profile is given by

$$\rho(r) = \frac{M}{4\pi}\frac{1}{r(r+a)^2}, \qquad \phi(r) = -\frac{GM}{r}\ln\left(1+\frac{r}{a}\right). \tag{2}$$

The Hernquist profile admits an analytic distribution function, but the NFW profile is a better fit to dark matter halos at large radii. We fit these profiles to our halo by matching the observed rotation curve of the galaxy, and

we also demand that the two models have the same coefficient to the $1/r$ core density profile. For the Hernquist profile we find that $M_{12} = M/(10^{12} M_\odot) = 3.78$ and $a_{\rm kpc} = a/(1\ {\rm kpc}) = 67.1$. The NFW profile has $M_{12} = 3.21$ and $a_{\rm kpc} = 43.8$.

We now define some useful quantities. We take $\mathcal{E} = \Psi(r) - v^2/2$ and $\Psi = -\phi$. We define dimensionless versions of the energy and potential, $\tilde{\mathcal{E}} = q^2 = a\mathcal{E}/(GM)$ and $\tilde{\Psi} = a\Psi/(GM)$. We also need a dimensionless density, which we define as $\tilde{\rho} = a^3\rho/M$.

Given that the sun moves through the halo at a velocity of 220 km sec^{-1} in the so-called ram direction, we need to know the distribution of relative velocities between clumps and the solar system as a function of the angle from the ram direction. Starting from the distribution function F, defined so that the mass in a phase space element is $dm = F d^3\mathbf{x}\, d^3\mathbf{v}$, we find that the number flux at the solar system is given by

$$\frac{\partial \mathcal{N}}{\partial v \partial \Omega} = \frac{1}{m_{\rm clump}} F v^2 v_{\rm rel}, \tag{3}$$

where $v_{\rm rel} = (v^2 + v_\odot^2 - 2 v v_\odot \mu)^{1/2}$, θ is the angle between the ram direction and the path of a given encounter, and $\mu = \cos\theta$. We also define $m_6 = m_{\rm clump}/(10^6 M_\odot)$. Note that a head-on collision has $\mu = -1$. We now transform the distribution functions to the solar system frame. To go from the relative velocity $v_{\rm rel}$ to the halo velocity v we must choose the correct sign. We find $v = v_\odot \mu \pm [v_{\rm rel}^2 - (1-\mu^2) v_\odot^2]^{1/2}$, and we must always take the positive root when $v_{\rm rel} > v_\odot$ to ensure that $v > 0$. Defining $v_{100} = v_{\rm rel}/(100\,{\rm km\ s^{-1}})$, we find that in the frame of the solar system, the number flux is

$$\frac{\partial^2 \mathcal{N}}{\partial v_{100} \partial \Omega} = \frac{3.25 \times 10^{-5}}{({\rm pc}^2\ {\rm Gy\ sr})} f M_{12}^{-1/2} m_6^{-1} a_{\rm kpc}^{-3/2} v_{100}^2 \left(\frac{v_{100}^2 + 4.84(2\mu^2 - 1)}{\sqrt{v_{100}^2 - 4.84(1-\mu^2)}} + 4.4\mu \right) \mathcal{F}(q). \tag{4}$$

The dimensionless part of the Hernquist distribution is

$$\mathcal{F}(q) = (1-q^2)^{-5/2} \left[3 \sin^{-1} q + q\sqrt{1-q^2}(1-2q^2)(8q^4 - 8q^2 - 3) \right] \tag{5}$$

and q is evaluated at the solar circle. The NFW profile does not have an analytic distribution function, but it can be evaluated numerically according to [12],

$$\mathcal{F}(q) = \int_0^{\tilde{\mathcal{E}}} \frac{d^2\tilde{\rho}}{d\tilde{\Psi}^2} \frac{d\tilde{\Psi}}{(\tilde{\mathcal{E}} - \tilde{\Psi})^{1/2}}. \tag{6}$$

The quantities $\tilde{\rho}$ and $\tilde{\Psi}$ are both known in terms of the parameter $u = r/a$, $\tilde{\rho} = u^{-1}(1+u)^{-2}$ and $\tilde{\Psi} = u^{-1}\ln(1+u)$. Again, q is evaluated at the solar circle.

We need to choose a reasonable size for the clumps. The galaxy would process an input spectrum of clump densities by disrupting all of the diffuse clumps, but simple calculations indicate that an overdensity of a factor of two over the total local density is easily safe from disruption [13]. We find that the size of a clump overdense by a factor of A is $r_{\rm clump} = 320(m_6/A)^{1/3}$ pc. We use $\pi r_{\rm clump}^2$ as the cross sectional area for purposes of determining the interaction rate. We define the effective interaction duration $T_{\rm int}$ as the time it takes the clump to cross the solar system at a velocity of 400 km s^{-1} times the overdensity A. We can use this quantity in Table I to determine the integrated signal of the encounter. We find $T_{\rm int} = 1.57(m_6 A^2)^{1/3}$ My.

We can now study the distribution of clump velocities as a function of direction. Multiplying equation (4) by the cross sectional area, we find the rate in terms of A. We set $m_6 = f = 1$, $A = 10$, and plot the distribution for four values of μ in Figure 1. In the forward direction, the peak of the distribution is at about 450 km s^{-1}, and as μ increases from -1 to 0, the position of this peak drops to about 300 km s^{-1}. The characteristic interaction time at the peak is roughly 25 $(m_6 A^2)^{1/3} f^{-1}$ My in the range $-1 < \mu < 0$.

The rate at which mica accumulates defects is a function of the angle α the incident particle makes with the cleavage plane. Monte Carlo simulations [5] of this process show that the rate of track accumulation dN/dt is well fit by the function

$$\frac{dN(\alpha)}{dt} = c_0 + c_1 |\cos\alpha|. \tag{7}$$

Experimental measurements using neutrons to simulate WIMPs are consistent with the etching model of the mica [11]. The constants c_0 and c_1 depend on the WIMP mass, the dispersion velocity of the halo, and the velocity of

the earth through the halo. They are calculated assuming that the mica has fixed orientation relative to the WIMP "wind". We are concerned with the signal contrast, defined as $s = (N_{\max} - N_{\min})/(N_{\max} + N_{\min})$, where the minimum and maximum N values are taken over all mica orientations on the earth. It is clear that the maximum possible signal contrast ω is given by $\omega = (1 + 2c_0/c_1)^{-1}$, though this can only be achieved if the mica has a fixed orientation over time. These constants have been computed for the standard halo [5]. To compute the relevant rates for the solar system interacting with a clump, we simply replace the virial and cutoff velocities of the halo with those of the clump. The velocity of the sun through the halo is replaced with the relative velocity in the interaction. We have computed these coefficients for several interaction velocities, in all cases taking the WIMP mass to be 100 GeV. The values are tabulated in Table I along with the results for an isothermal halo. The values all assume a density of 0.3 GeV cm^{-3}, so they must be weighted appropriately by the density of the clump. These results are insensitive to the virial and cutoff velocities because the velocities of the collisions we consider are much higher than the thermal velocities.

We need to account for the motion the mica sample makes through the galaxy. The rotation of the earth with a period of one sidereal day and the precession of the equinoxes with a period of 25,800 years are both very rapid compared to any timescale we are concerned with, so we average over these motions. The two motions that we are more concerned with are the galactic orbit and tectonic drift. The galactic year is about 225 My, and the motion of the continents occurs on timescales of 10-100 My. All of these effects are taken into account in computing the total track accumulation in a sample of mica as a function of its age, continent, and orientation. The remaining directional signal from the isothermal halo is typically at the 1% level [5].

We now discuss the effect of a clump encounter at some time in the past on the observed track density. As our example, we consider mica that is 440 My old, two galactic years. Clearly we have some freedom in choosing the parameters m_6, A, and f to give an interaction rate of this order. Conversely, we can also sample mica at different ages to roughly measure the interaction rate. Realistically, we can cover two orders of magnitude in interaction rate by choosing mica of ages 10-1000 My.

We compute the track accumulation in the sample for the standard halo. We then compute the track accumulation due to a single $10^6 M_\odot$ clump interacting at various times between the mica formation and the present. Because the clump encounter happens quickly, we may neglect the effects of galactic orbit and tectonic drift during the encounter, but we must still average over the diurnal rotation and the precession of the equinoxes. When properly weighted, we can simply add on the contribution of the nearly instantaneous clump encounter to the isothermal result to produce the final map. We can predict the signal contrast and also the directions of minimum and maximum track accumulation. We take a conservative approach and add the clump encounter to a standard halo of full density. This illustrates that the clump encounters can be seen even if they make up only a small fraction of the mass in the halo. For $A = 10$, the change in signal can be substantial. Some of the forward solid angle sees a significant change in signal, but a large part sees only a small difference. At $A = 100$ the signal is much more promising. Most of the forward solid angle shows a pronounced change in the signal, both in that the signal contrast is several times larger, and in that the maximum and minimum directions are very different than the no encounter case. When we take $A = 1000$ the difference in signal is quite large. The signal contrast is as much as ten times larger than the no interaction case. The signal contrasts are listed in Table II, and we plot some example sky maps for mica located near the center of the North American craton to illustrate these differences in Figure 2. In the table and plots we assume that the isothermal signal is at full strength, thus the signal can only improve as f increases from zero. We have noticed that the signal from a clump encounter 440 My ago seems to be oriented in the same direction for all incident directions. This is due to the fact that the North American craton was on the equator at this time, and the signal can have no dependence on the right ascension. For encounters occurring 220 My ago, this degeneracy is broken since the continent has moved away from the equator.

The problem of recovering the details of a clump encounter is very much overconstrained. We can sample mica of different ages, different orientations, and different continents to obtain a large amount of information about the encounter. The discovery of a signal can be verified with a high degree of confidence by using other mica samples.

In summary, we stress the main point of this Letter. Using mica as a WIMP detector has the two advantages of direction sensitivity and integration times as long as 1 Gy. These two properties can be used to discover substructure in the cold dark matter halo of the galaxy. The hierarchical clustering paradigm of structure formation in the universe suggests that substructure may well persist in the halo, so this is an important experimental program. In fact, substructure in the halo may make unambiguous detection of halo WIMPs easier because of the larger directional signal provided.

We would like to thank J. Silk and A. Burkert for useful discussions and comments on the manuscript. This research was supported in part by grants from NASA and DOE.

[1] V. Trimble, Ann. Rev. Astron. Astrophys. **25**, 425 (1987)
[2] G. Jungman, M. Kamionkowski, and K. Griest, Phys. Rep. **267**, 195 (1996) and references therein.
[3] D. P. Snowden-Ifft, E. S. Freeman, and P. B. Price, Phys. Rev. Lett. **74**, 4133 (1995).
[4] D. P. Snowden-Ifft and M. K. Y. Chan, Nucl. Instrum. Methods B **101**, 247 (1995).
[5] D. P. Snowden-Ifft and A. J. Westphal, Phys. Rev. Lett. **78**, 1628 (1997).
[6] W. H. Press and P. Schechter, Astrophys. J. **187**, 425 (1974); C. Lacey and S. Cole, Mon. Not. R. Astron. Soc. **262**, 627 (1993); **271**, 676 (1994).
[7] K. V. Johnston, astro-ph/9710007 (1997).
[8] A. Burkert and J. Silk, private communication
[9] L. Hernquist, Astrophys. J. **356**, 359 (1990).
[10] J. F. Navarro, C. S. Frenk, and S. D. M. White, Mon. Not. R. Astron. Soc. **275**, 720 (1995); Astrophys. J. **462**, 563 (1996); (to be published) astro-ph/9611107.
[11] D. P. Snowden-Ifft and E. S. Rykoff, unpublished
[12] J. Binney and S. Tremaine, *Galactic Dynamics* (Princeton University Press, Princeton, 1987).
[13] E. R. Capriotti and S. L. Hawley, Astrophys. J. **464**, 765 (1996).

FIG. 1. Observed number flux of clumps interacting with the earth as a function of arrival direction and velocity. We take $m_6 = f = 1$ and $A = 10$. Both Hernquist and Navarro, Frenk, and White profiles are shown. It is clear that there is very little difference between the two.

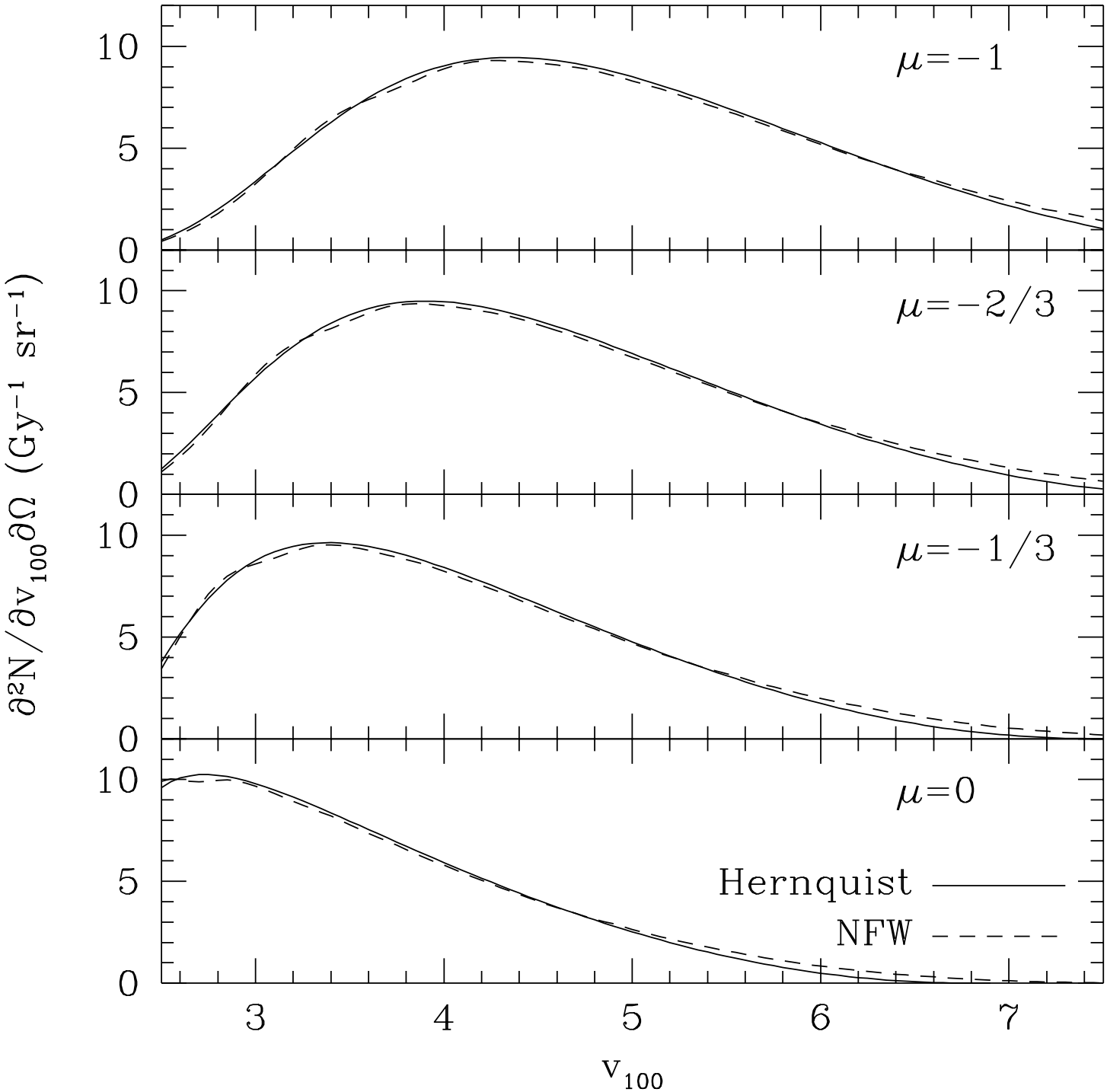

FIG. 2. Track accumulation as a function of present day mica orientation. We illustrate the background signal (dashed) along with four clump encounters at various ages (solid). The background signal contrast of 0.0291 can be compared with the signal in each plot. *Top left:* $A = 10$, 440 My, ram direction. *Top right:* $A = 100$, 220 My, 60 degrees north of the ram direction. *Bottom left:* $A = 100$, 275 My, 30 degrees south of the ram direction. *Bottom right:* $A = 1000$, 275 My, 60 degrees west of the ram direction.

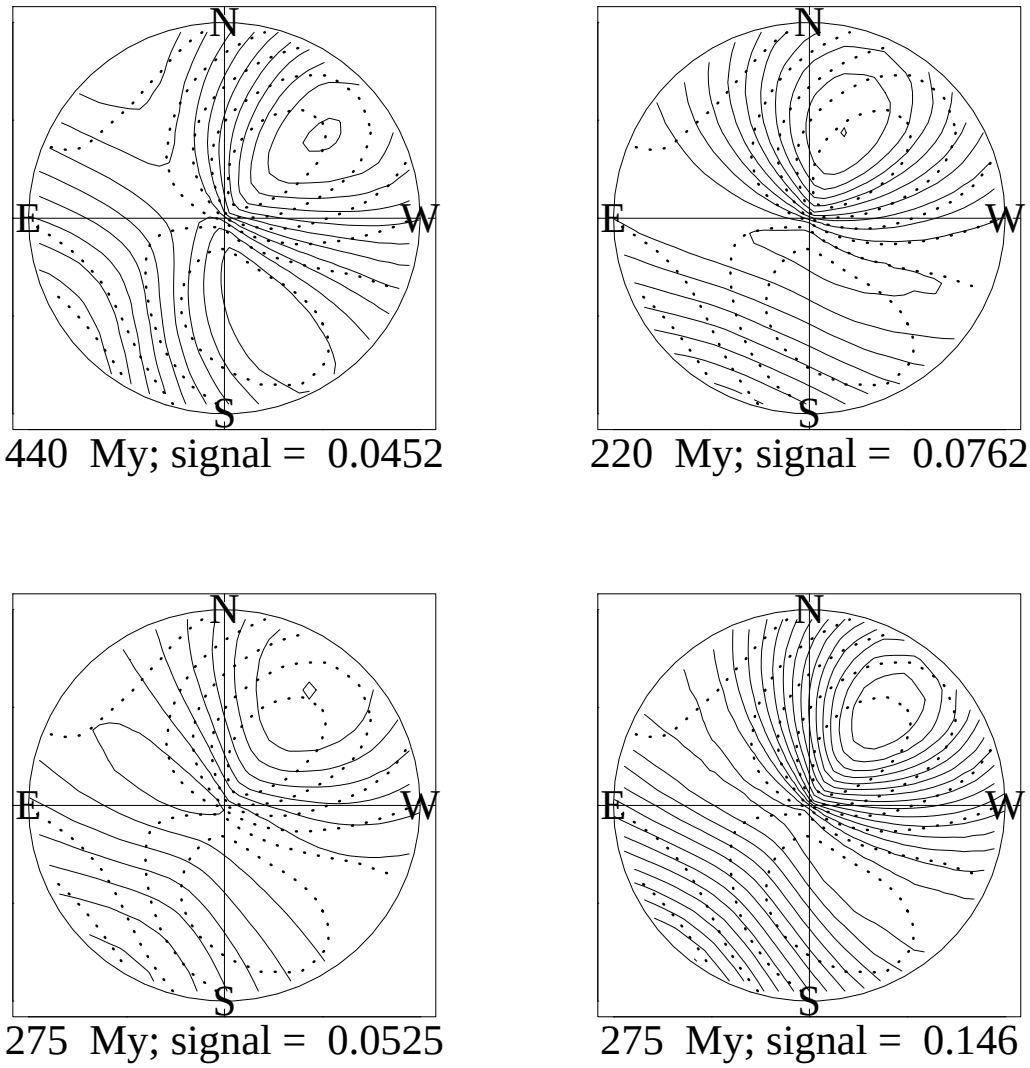

TABLE I. Track accumulation rate coefficients c_0 and c_1 and signal contrast ω for several interaction velocities. The values for the standard isothermal halo are also given. The WIMP mass is taken to be 100 GeV.

Velocity (km s^{-1})	c_0 (cm^{-2} Gy^{-1})	c_1 (cm^{-2} Gy^{-1})	ω
300	-16 700 ± 43 000	370 000 ± 61 000	1.10 ± 0.28[a]
400	550 000 ± 200 000	1 800 000 ± 290 000	0.62 ± 0.094
500	4 800 000 ± 360 000	1 500 000 ± 500 000	0.14 ± 0.04
600	12 700 000 ± 500 000	-700 000 ± 740 000	-0.03 ± 0.03
700	27 400 000 ± 960 000	-7 300 000 ± 1 400 000	-0.15 ± 0.03
halo	2 860 000 ± 80 000	700 000 ± 100 000	0.11 ± 0.001

[a]Note that $|\omega| > 1$ is unphysical, but in this case the 1σ error bars cover unity so we set $\omega = 1$

TABLE II. Signal contrast for encounters with a $10^6 M_\odot$ clump in mica 440 My old. The clump overdensity A and encounter time in My are listed with the arrival direction relative to the ram direction in galactic coordinates. Clumps coming from the galactic center and north galactic pole are also listed.

Direction	$A = 10$			$A = 100$			$A = 1000$		
	220	275	440	220	275	440	220	275	440
no clump	0.0291	0.0291	0.0291	0.0291	0.0291	0.0291	0.0291	0.0291	0.0291
ram	0.0446	0.020	0.0452	0.102	0.0573	0.106	0.229	0.189	0.233
pole	0.0286	0.0284	0.0285	0.0268	0.0260	0.0265	0.0217	0.0195	0.0240
center	0.0274	0.0316	0.0279	0.0236	0.0412	0.0255	0.0424	0.0833	0.0497
30°E	0.0394	0.0211	0.0388	0.0792	0.0345	0.0809	0.172	0.125	0.175
30°S	0.0259	0.0201	0.0255	0.020	0.0525	0.0248	0.0412	0.177	0.0456
30°W	0.0336	0.0252	0.0319	0.0533	0.0182	0.0522	0.102	0.0303	0.103
30°N	0.0550	0.0209	0.0569	0.143	0.0368	0.151	0.332	0.131	0.342
60°E	0.0272	0.0330	0.0268	0.0226	0.0473	0.0223	0.0261	0.0891	0.0304
60°S	0.0237	0.0238	0.0255	0.0419	0.0204	0.0489	0.148	0.0807	0.152
60°W	0.0250	0.0372	0.0256	0.0269	0.0662	0.0336	0.0969	0.146	0.102
60°N	0.0380	0.0257	0.0381	0.0762	0.0190	0.0785	0.186	0.0366	0.191